Breast Cancer: Targets and Therapy

Dovepress
Taylor & Francis Group

Open Access Full Text Article

ORIGINAL RESEARCH

Effects of *Clinacanthus nutans* Extracts on Cell Proliferation and Apoptosis in Triple-Negative Breast Cancer: Mechanistic Insights

Jiafang Xu[1,*], Jincha Long[2,*], Zhen ying Li[3,*], Chaoqun Wang[4], Yonggang Zhang[5], Huifang He[2], Qingjie Hu[2], Siqi Yin[2], Hai Li[2], Naizhen Wang[2], Qiang Gao[2], Shuaining Tang[2], Yongkang Zhu[6], Peng Wang[3], Renjun Feng[3], Yu Liu[2,6]

[1]Reproductive Medicine Center, The First Affiliated Hospital of Hainan Medical University, Haikou, People's Republic of China; [2]Department of Breast Surgery, The First Affiliated Hospital of Hainan Medical University, Haikou, People's Republic of China; [3]Key Laboratory of Tropical Translational Medicine of Ministry of Education & Key Laboratory of Brain Science Research Transformation in Tropical Environment of Hainan Province, School of Basic Medicine and Life Sciences, Hainan Medical University, Haikou, People's Republic of China; [4]Department of Nuclear Medicine, Hainan General Hospital, Hainan Affiliated Hospital of Hainan Medical University, Haikou, People's Republic of China; [5]Department of General Surgery, People's Hospital of Rizhao, Rizhao, People's Republic of China; [6]Department of General Surgery, Nanjing University of Chinese Medicine Affiliated Hospital, Nanjing, People's Republic of China

*These authors contributed equally to this work

Correspondence: Yu Liu, Department of Breast Surgery, The First Affiliated Hospital of Hainan Medical University, Haikou, People's Republic of China, Email 15218046@qq.com; Renjun Feng, Department of General Surgery, Nanjing University of Chinese Medicine Affiliated Hospital, Nanjing, People's Republic of China, Email hy0206183@muhn.edu.cn

Objective: To explore the effects of *Clinacanthus nutans* extract (CnE) on triple-negative breast cancer (TNBC) and mechanism of action.

Methods: In vitro, the human TNBC cell lines were treated with the extract at various concentrations. Cell viability was assessed using the CCK8 assay. In vivo, establishing a subcutaneous xenograft tumor model of TNBC, Hematoxylin-eosin staining and TUNEL assay were used to evaluate the effect of CnE on tumor proliferation. Tumor proteins were extracted, Quantitative proteomics and subsequently analyzed using bioinformatics approaches. Finally, immunohistochemistry evaluates the protein expression differences of ATP2A3, PLA2G4A, and ITPK1.

Results: In vitro, CnE inhibited TNBC cell proliferation in a concentration-dependent manner, with IC50 values of 420 ± 35 μg/mL (MDA-MB-231) and 380 ± 28 μg/mL (MDA-MB-468), showing maximal 68.5% inhibition at 800 μg/mL ($p < 0.001$). The TNBC xenograft model was successfully established, and tumours in the extract-treated group were markedly smaller than those in the saline group. On day 28, the tumour inhibition rate was 28.66%, significantly higher than that in the saline group ($P < 0.05$). Haematoxylin–eosin staining staining and TUNEL assay showed increased tumor necrosis and apoptosis induction.($P < 0.001$). Proteomic analysis showed that among the 4,908 identified proteins, 80 were upregulated, and 7 were downregulated. Bioinformatics analysis indicated involvement in the extracellular matrix, fatty acid metabolism, cell apoptosis, ferroptosis, immune response, choline metabolism, and amino acid metabolism. Immunohistochemistry revealed increased expression of ATP2A3 (1.3-fold, $p < 0.05$), PLA2G4A (1.6-fold, $p < 0.05$) and ITPK1 (3.2-fold, $p < 0.01$) proteins in the extract group compared to the control group.

Conclusion: CnE inhibits TNBC cell proliferation, suppresses tumor growth, The mechanism likely involves multiple biological processes and pathways, Key pathways included apoptosis, ferroptosis, and necroptosis signaling.

Keywords: *Clinacanthus nutans*, triple-negative breast cancer, proteomics, ATP2A3, PLA2G4A, ITPK1

According to Cancer Statistics 2024, the number of new breast cancer cases is projected to reach 2.3 million, ranking second only to lung cancer. Annual mortality is estimated at 670,000 cases, making it the fourth leading cause of cancer-related death worldwide, surpassing stomach cancer.[1] Breast cancer encompasses various molecular subtypes,

Received: 14 March 2025
Accepted: 16 August 2025
Published: 15 September 2025

including triple-negative breast cancer (TNBC), which accounts for approximately 15–20% of all invasive breast cancer cases and exhibits high heterogeneity.[2] TNBC is characterised by aggressive invasiveness, rapid growth and spread, poor prognosis, early onset and high metastatic potential compared with other subtypes. Lacking effective therapeutic targets, TNBC is resistant to endocrine and targeted therapies and has a high recurrence and mortality risk. Consequently, chemotherapy remains the primary treatment, although its efficacy is limited. The 5-year survival rate is below 30%, with a median progression-free survival of 2.9–7.7 months and a median overall survival of approximately 13 months. Patients have a poor prognosis[3] and numerous adverse effects, leading to poor tolerance.[4] These challenges underscore the urgent need for more effective strategies to improve TNBC treatment outcomes and patient quality of life.

In traditional Chinese medicine, breast cancer has historically been described as "mammary cancer", "stiff carbuncle" or "breast nodes", among other terms, with records tracing back to "Miraculous Pivot". According to the "Orthodox Manual of External Medicine", its aetiology is described as follows:

> depression and sadness damaged the liver, overthinking hurt the spleen, while long-term continuous thinking would have a negative impact on the heart. Those who wished but failed to achieve their goals would experience meridian blockage and develop nodes., known as mammary cancer.

Clinacanthus nutans (*C. nutans*) is a plant from the Acanthaceae family that is widely distributed in Malaysia, Indonesia, Thailand and southern to southwestern China (eg Guangdong, Guangxi and Yunnan).[5] First documented in the "List of Medicinal Plants in Guangxi", its whole plant or leaves are used medicinally. With a sweet and slightly bitter taste and a cool nature, it targets liver and kidney meridians. Its functions include clearing heat and dampness, inducing diuresis and reducing oedema, promoting blood circulation, unblocking meridians and preventing tumours.[6] In recent decades, *C. nutans* has gained popularity in Southeast Asia, where patients with cancer in Malaysia have reported its anti-tumour effects. Modern pharmacological studies have confirmed that its chemical constituents, including triterpenoids, flavone C-glycosides, glucosides and glucosinolates, exhibit anti-tumour activity.[7,8] Malaysian researchers have demonstrated its inhibitory effects on cancer cell lines. For instance, at a mass concentration of 100 μg/mL, the chloroform extract of *C. nutans* inhibited human leukaemia (K562), lymphoma (Raji) and liver cancer (HepG2) cell lines at rates of 91.28% ± 0.03%, 88.97% ± 1.07% and 41.88% ± 2.81%, respectively. The extract also exerted inhibitory effects on lung (NCL-H23), gastric (SNU-1), cervical (HeLa) and colon (LS-174T) cancer cell lines, indicating strong anti-tumour potential.[9] Yusmazura et al observed a pronounced toxic effect of the aqueous CnE on HeLa cells,[10] and Ghasemzadeh et al[11] found that methanol extracts from 6-month-old buds significantly reduced HeLa cell viability.[12]

Despite its demonstrated anti-tumour effects, little is known about the impact of CnE on breast cancer or its specific molecular mechanisms. Therefore, this study aimed to investigate the effects and mechanisms of CnE on TNBC cell proliferation and apoptosis, thereby providing theoretical insights and data to support clinical drug development.

Materials and Methods

Animals and Cells

The experimental animals were 6- to 8-week-old female M-NSG mice (n = 23, weighing approximately 18–20 g) provided by Shanghai Model Organisms Center, Inc. (production license no.: SCXK (Shanghai) 2019–0002. The animals were housed at the Animal Experiment Center of Nanjing University of Chinese Medicine under controlled conditions (20°C–22°C, 40–60% relative humidity and a 12-h light–dark cycle, with continuous purification and ventilation comprising 10 changes per hour). Animals had free access to feed and water, with the feed and bedding uniformly sourced by the experimental centre. All animal experiments were approved by the Institutional Animal Care and Use Committee of Hainan Medical University (Approval No: HYLL-2023-355) and conducted in compliance with the National Regulations for the Administration of Laboratory Animals in China (2017 Revision) and the NIH Guide for the Care and Use of Laboratory Animals (8th edition, 2011). The human TNBC cell lines MDA-MB-231 and MDA-MB-468 were obtained from FuHeng Biology (Shanghai, China).

Drugs

The dried leaves of *C. nutans* (CNE-2023-03) were purchased from Hainan Bohe Agricultural Development Co., Ltd.

Reagents and Equipment

Reagents

50 mLTube (430828), 10mL Tube (430167), 10 cm Dish, 15 mL tube (430167), 10 mL Stripette (SP-003-10), Matrigel (354234), and L-15 (10–045-CV) were from Corning, PBS (10010–023) and 0.25% (w/v) Trypsin-0.53 mM EDTA (2360155) were from Gibco, HBSS (B420KJ) was from Basalmedia, FBS (SFBS) was from BOVOGEM, 75% disinfection alcohol (801769610) was obtained from China National Pharmaceutical Group Corporation, Urea (BIO-RAD, 161–0731), SDS (sangon biotech, SB0485-500g), Tris (sangon biotech, T0826-500g), iodoacetamide (IAA, Sigma, I1149-5G), C18 Empore™ solid-phase extraction disc (Sigma, 66883-U), BCA Quantitative Kit (Beyotime Biotechnology, P0012), NH_4HCO_3 (Sigma, A6141-25G), Formic acid (Thermo Fisher Scientific, A117), acetonitrile (Merck, 1000304008), C18 Cartridge (Waters, WAT023590), Acetyl-Lysine Motif [Ac-K] Kit (Cell Signaling Technology,13416S), 1M TEAB (Thermo SE252676/90,114), Thermo Scientific High SelectTM Top14 Abundant Protein Depletion Mini Spin Columns (Thermo), SDS-PAGE protein loading buffer (Beyotime Biotechnology, P0015F), Lysing Matrix A(MP, 6910–100-99,219), dithiothreitol (DTT, Sigma, 43819–5G), HCOONH4 (Sigma, 17843), NH_3•H_2O (Sigma, 17837), HCl (Sinopharm, 10011018), BSA (Sangon, A0332), Trypsin (Promega, V5117), Trifluoroacetic acid (TFA, Sigma, T6508), 30kD ultrafiltration centrifuge tube (Sartorius, VN01H22), 0.22 μm ultra-filtration centrifuge tube (Corning Spin-X, 8160), Multiple Affinity Removal LC Column-Human 14 / Mouse 3 (Agilent), Immunohistochemistry kit purchased from Beijing leagene biotech, TUNEL kit was purchased from Tangshan Yingsheng Biotechnology, CCK-8 reagent was purchased from Shanghai Beyotime Biotechnology Co, LTD, Hematoxylin and eosin staining solutions were purchased from Beijing leagene biotech.

Methods

Preparation of the Clinacanthus nutans Extract (CnE)

To prepare 5 L of 85% ethanol, 4.25 L of 100% anhydrous ethanol was mixed with 0.75 L of distilled water. Subsequently, 900 g of *C. nutans* aerial parts, naturally shade-dried (100 g retained), were soaked in 85% ethanol at room temperature. The mixture was fully immersed every 7 days and extracted three times with the solutions combined. The concentrated solution was dried by rotary evaporation to obtain a viscous brown extract. The extract was prepared on-site at the required concentrations for further use. When administered, complete culture medium is used to dilute to the required concentration.

Cell Experiments

Cell Culture

The human breast cancer cell lines MDA-MB-231 and MDA-MB-468 were cultured in a high-glucose medium (DMEM) containing 10% fetal bovine serum in a 5% CO_2 incubator at 37°C. When cells reached 80–90% confluence, they were digested and passaged. Cells in the logarithmic growth phase were used in subsequent experiments.

Cell Viability Testing

MDA-MB-231 and MDA-MB-468 cells in the logarithmic growth phase were digested and counted to prepare a suspension with a concentration of 1.5×10^5/well, which was seeded into a 96-well plate. The experimental groups included a control group (cells without extract treatment but normal culture medium), a blank group (treated with cell-free culture medium) and CnE groups treated with extract gradient concentrations of 200, 400, 600, 800 and1000 μg/mL. After 24 h of incubation, the original culture medium was replaced with fresh medium and the corresponding concentrations of CnE, followed by an additional 48 h of incubation. CCK8 solution was then added, and after 1 h of incubation, optical density was measured using a multifunctional microplate reader. Cell viability was calculated to determine the optimal concentration of CnE for further intervention in MDA-MB-231 and MDA-MB-468 cells.

IC50 values were determined by nonlinear regression analysis (four-parameter logistic model) using GraphPad Prism 9.0: Y = Bottom + (Top - Bottom)/(1 + 10^((LogIC50 - X)*Hill Slope). where Top and Bottom represent maximum and minimum viability plateaus, respectively. Three independent experiments yielded IC50 values of 420 ± 35 μg/mL (MDA-MB-231) and 380 ± 28 μg/mL (MDA-MB-468).

Animal Experiments

Modelling, Grouping and Medication

MDA-MB-231 cells in the logarithmic growth phase were harvested, resuspended in Hank's Balanced Salt Solution and counted to adjust the cell density to 5×10^7 cells/mL. A 0.2-mL tumour cell suspension (containing 50% Matrigel) was subcutaneously injected near the dorsal right forelimb of each mouse, delivering 5×10^6 cells per mouse. Once tumours reached 150–200 mm^3, 15 mice were randomly selected and divided into two groups based on tumour volume: seven in the saline group and eight in the CnE group. Mice were gavaged with either 0.9% saline or CnE for 28 consecutive days.

Tumour Detection in Mice

From the initiation of modelling to the end of treatment, subcutaneous tumour volume was measured weekly, and tumour growth curves were plotted. After treatment, tumours were excised and weighed to calculate the tumour inhibition rate.

Pathological Examination and TUNEL Assay

Pathological examination of tumour tissues was performed using HE staining. Tumour cell apoptosis was assessed using the TUNEL kit according to the manufacturer's instructions.

Extraction of Protein from Xenograft Tumour Tissue

Xenograft tumour tissues were homogenised with SDT lysis buffer in Lysing Matrix A tubes using an MP homogeniser (24 × 2, 6.0 M/s, 30s, twice). The homogenate was then subjected to ultrasonication, boiled for 10 min and centrifuged at 14,000 g for 15 min. The supernatant was filtered through a 0.22-μm filter tube, and the protein concentration was measured using BCA. Aliquots of samples were stored at −80°C.

Sodium Dodecyl-Sulphate Polyacrylamide Gel Electrophoresis

Protein samples (20 μg per sample) were mixed with 6× loading buffer, boiled for 5 min and resolved using 12% sodium dodecyl-sulphate polyacrylamide gel electrophoresis at 250 V for 40 min. Proteins were stained with Coomassie Blue.

Filter-Aided Sample Preparation

For each sample, 100 μg of protein solution was mixed with dithiothreitol to a final concentration of 100 mM, boiled for 5 min and cooled at room temperature. The solution was combined with 200 μL of UA buffer and centrifuged in a 30-kD ultrafiltration tube at 12,500 g for 15 min, after which the filtrate was discarded. After a second centrifugation, 100 μL of indole-3-acetic acid (IAA) buffer (100 mM IAA in UA) was added, vortexed at 600 rpm for 1 min and incubated in the dark for 30 min. Following another centrifugation at 12,500 g for 15 min, the filter was washed with 100 μL of UA buffer, and this process was repeated twice. After adding 100 μL of 50 mM NH_4HCO_3 solution, centrifugation was performed at 12,500 g for 15 min, and this process was repeated twice. The solution was then transferred to a new tube and mixed with 40 μL of Trypsin buffer (4 μg of Trypsin in 40 μL of 50 mM NH_4HCO_3 solution). After vortexing at 600 rpm for 1 min, samples were incubated at 37°C for 16–18 h. Peptides were collected after centrifugation at 12,500 g for 15 min, with 40 μL of 50 mM NH_4HCO_3 solution added for further centrifugation at 12,500 g for 15 min to collect the filtrate. Peptide fragments were then desalinated using a C18 cartridge, freeze-dried and finally resuspended in 40 μL of 0.1% formic acid for quantification at OD280.

Mass Spectrometric Analysis

Samples were separated using an Easy-nLC system with a nanolitre flow rate. Buffer solution A consisted of 0.1% formic acid in water, whereas buffer solution B consisted of 0.1% formic acid in 80% acetonitrile. The chromatographic column was equilibrated with Buffer A. Samples were loaded via an automatic sampler and separated on an analytical column (Acclaim PepMap RSLC 50 μm × 15 cm, NanoViper, P/N164943; Thermo Fisher Scientific) at 300 nL/min.

Following chromatographic separation, mass spectrometric analysis was performed using an Orbitrap Exploris 480 system for 90 min (depending on the specific experimental protocol). The detection mode was positive ion with a parent ion scanning range of 350–1,200 m/z, primary mass resolution of 120,000, automatic gain control (AGC) target of 300%, and primary maximum injection time of 50 ms. Peptides and fragments were analysed in data-dependent mode with a 1.5-s cycle time, using higher-energy collisional dissociation as the tandem mass spectrometry activation type, a 1.6-m/z isolation window, a 75% AGC target, 15,000 as the secondary mass spectrometry resolution, one microscan, a 35-ms secondary maximum injection time, a 30-s ion dynamic exclusion time and 33% normalised collision energy.

Protein Identification and Quantification

Mass spectrometry data were analysed using the *Rattus norvegicus* protein database (RefSeq) from the NCBI database. Raw files were processed using MaxQuant software (version 1.6.17.0) for database searching and data analyses. Trypsin/P was set as the cleavage enzyme, allowing up to two missed cleavages. Methionine oxidation was set as a variable modification, with cysteine iodoacetylation and TMT modifications being fixed. The parent ion mass tolerance was 15×10^{-5}, and the daughter ion tolerance was 0.02 Da. The false discovery rates of peptide and protein identification were set to 0.01. Differentially expressed proteins were screened using a fold-change cut-off of 2.0 and a P-value threshold of 0.5 for relative quantification.

Bioinformatics Analysis

After obtaining the raw mass spectrometry files, a sample-specific protein database was constructed based on the sample source. This database was analysed using specialised software, followed by quality control at the peptide fragment and protein levels. After validating the mass spectrometry data, the subsequent steps included a repeatability test of the sample quantification results, significant difference analysis and bioinformatics investigation. Gene Ontology (GO) and pathway functional enrichment analyses were conducted using genes corresponding to differentially expressed proteins. Relevant databases for protein function annotation included the Kyoto Encyclopedia of Genes and Genomes (KEGG), Reactome, BioCyc, PANTHR and PID. Protein–protein interaction (PPI) network analysis for differentially expressed proteins was performed using the STRING platform (www.string-db.org) and Cytoscape software.

Pan-Cancer Prognostic Analysis

Pan-cancer prognostic analysis was conducted using data from The Human Protein Atlas website (https://www.proteinatlas.org/). The survival curves were generated using GraphPad Prism 8.

Histopathology Analysis

To evaluate tumor cell morphology, hematoxylin and eosin (HE) staining was performed in this study.[13] The expression levels of ATPase sarcoplasmic/endoplasmic reticulum Ca2+ transporting 3 (ATP2A3), Phospholipase A2 Group IVA (PLA2G4A), and inositol 1,3,4-trisphosphate 5/6-kinase (ITPK1) proteins were analyzed using an Immunohistochemical (IHC) staining kit according to the manufacturer's instructions.

Statistical Analysis

Data analysis and visualization for this study were conducted using SPSS 27 and GraphPad Prism 8. Continuous data following a normal distribution are presented as means ± standard deviations. Statistical analyses were performed using either a one-way analysis of variance or a two-tailed Student's *t*-test, depending on the homogeneity of variance. A P-value of <0.05 was considered statistically significant.

Results

CnE Inhibits the Viability of MDA-MB-231 and MDA-MB-468 Cell Lines

The CCK8 assay was employed to assess the effects of CnE on the viability of MDA-MB-231 and MDA-MB-468 cell lines. Compared to the control group, the cell proliferation rates in the extract group decreased in a concentration-

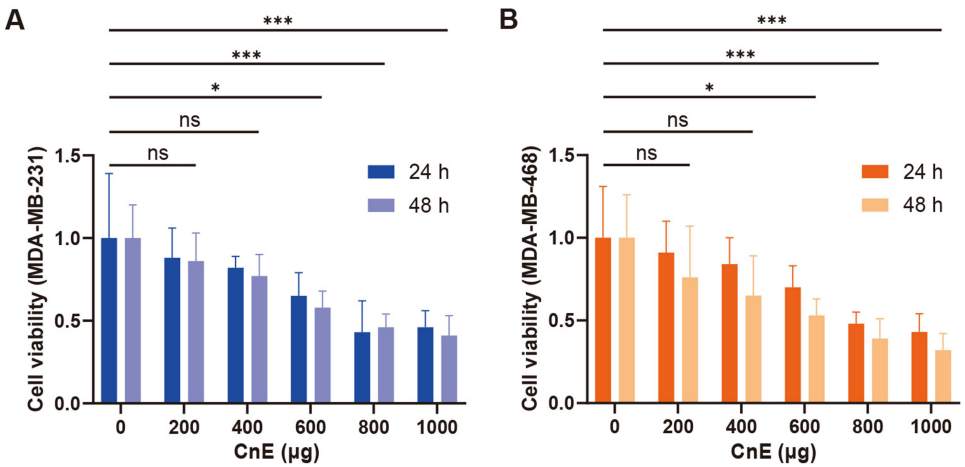

Figure 1 Effects of CnE on the viability of MDA-MB-231 and MDA-MB-468 cell lines. (**A**) Viability of MDA-MB-231 cell line (n = 5). (**B**) Viability of MDA-MB-468 cell line (n = 5). Data are presented as mean ± SEM. Statistical significance was determined using an unpaired, two-tailed Student's *t*-test. **P* < 0.05, ***P* < 0.01, ****P* < 0.001; ns indicates not significant.
Abbreviation: CnE, *Clinacanthus nutans* extract.

dependent manner (Figure 1). Notably, the 800 μg/mL concentration of CnE resulted in the most significant reduction in cell numbers for both cell lines. This concentration also corresponds to their IC50 value.

CnE Inhibits the Growth of Subcutaneous Tumors in TNBC Model in Mice

To assess the impact of CnE on tumour growth, tumour volumes and weights were measured before and after administration. In this study, a subcutaneous tumor model (TNBC model) was established using MDA-MB-231 cells in M-NSG mice. The tumor volumes (Figure 2B) and weight changes (Figure 2C) indicated that on day 28, the mean tumor volume in the extract group (546.1 ± 29.09 mm^3) was significantly lower than that in the saline group (702.63 ± 45.21 mm^3), with $p < 0.01$. The average tumor weight of the extract group (0.638 ± 0.034 g) was significantly lower than that of the saline group (0.737 ± 0.047 g) with statistical significance ($p < 0.001$). Xenograft tumors were successfully formed in all mice, resulting in a tumor formation rate of 100%. Interestingly, the extract group exhibited a significantly lower body weight than the saline group (Figure 2D), with $p < 0.001$. This suggests that the extract may have accelerated fat metabolism in the xenograft tumor model mice, leading to reduced body weight.

Proteomic Analysis of Subcutaneous Tumors

Analysis of Differentially Expressed Proteins

Proteomic analysis using label-free mass spectrometry identified 4,908 proteins in tumour tissues. Based on the screening criteria ($|\log2FC| \geq 1.5$ and $P < 0.05$), 87 differentially expressed proteins were identified (Figure 3A and B, Supplementary Table 1), including 80 upregulated and 7 downregulated proteins in the CnE-treated group compared with the control group.

GO Enrichment Analysis of Differentially Expressed Proteins

GO enrichment analysis (Figure 3C) indicated that the differentially expressed proteins were primarily associated with the extracellular matrix, extracellular space, and collagen type I trimer, which were enriched in the cell component category. In the molecular function category, the differentially expressed proteins were enriched for functions related to iron ion binding, oxygen binding, and oxygen carrier activity. The differentially expressed proteins were also primarily associated with collagen fibril organization, regulation of protein complex assembly, and oxygen transport in the biological process category.

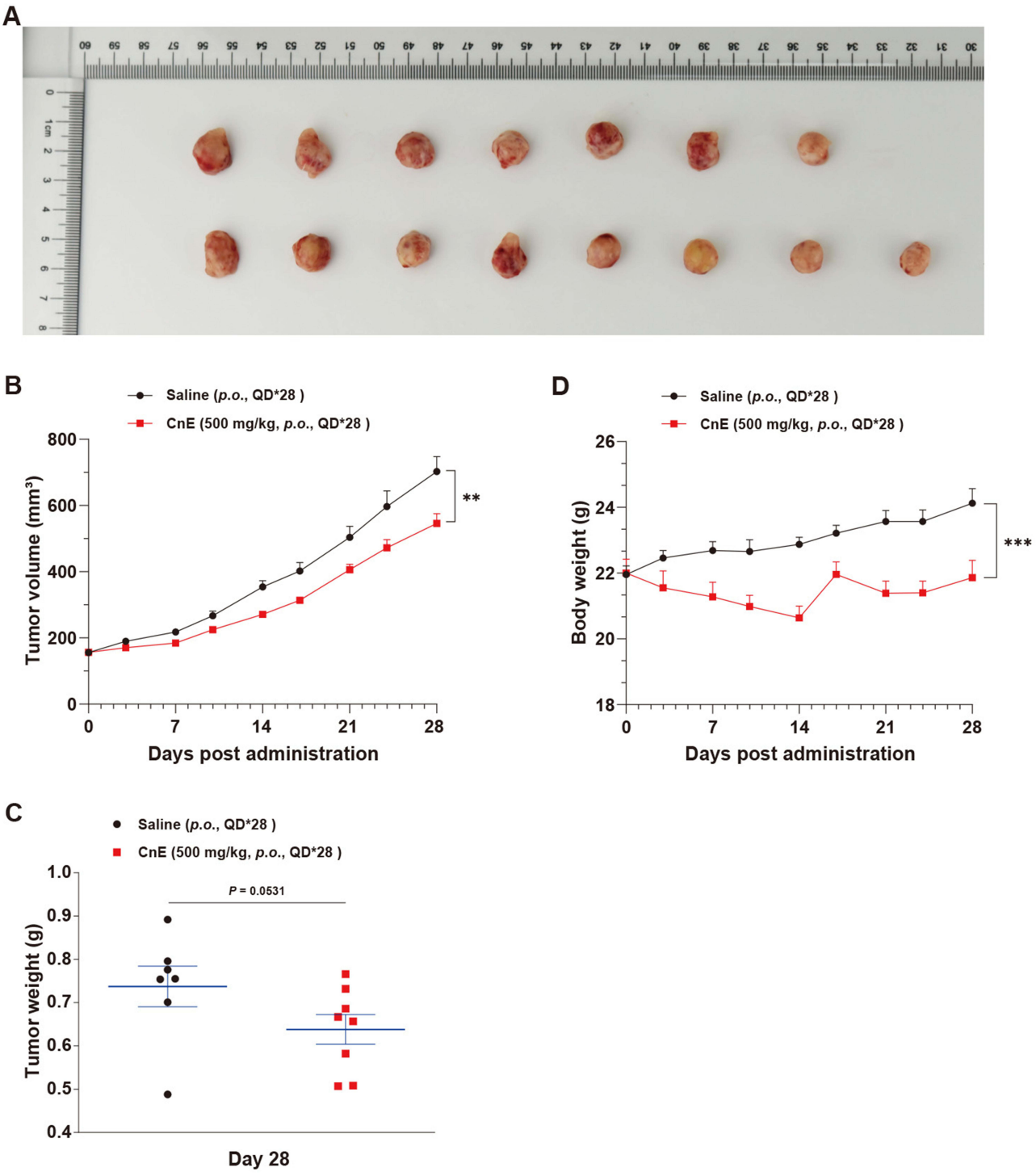

Figure 2 Effect of CnE on subcutaneous tumors in the TNBC model mice. (**A**) Tumor images; (**B**) Tumor volume; (**C**) Tumor weight; (**D**) Mice body weight. The treatment group received CnE at a dose of 500 mg/kg, while the control group was given 500 mg/kg saline. The endpoint for drug administration was 28 days. Saline group (n=7), CnE group (n=8). Data are presented as mean ± SEM. Statistical significance was determined using an unpaired, two-tailed Student's *t*-test. **P* < 0.05, ***P* < 0.01, ****P* < 0.001; ns indicates not significant.

Abbreviations: CnE, *Clinacanthus nutans* extract; TNBC, triple-negative breast cancer.

KEGG Enrichment Analysis of Differentially Expressed Proteins

KEGG pathway analysis (Figure 3D) revealed that, compared to the control group, the differentially expressed proteins in the CnE group were associated with pathways related to unsaturated fatty acid metabolism (eg, linoleic acid metabolism,

https://doi.org/10.2147/BCTT.S528242

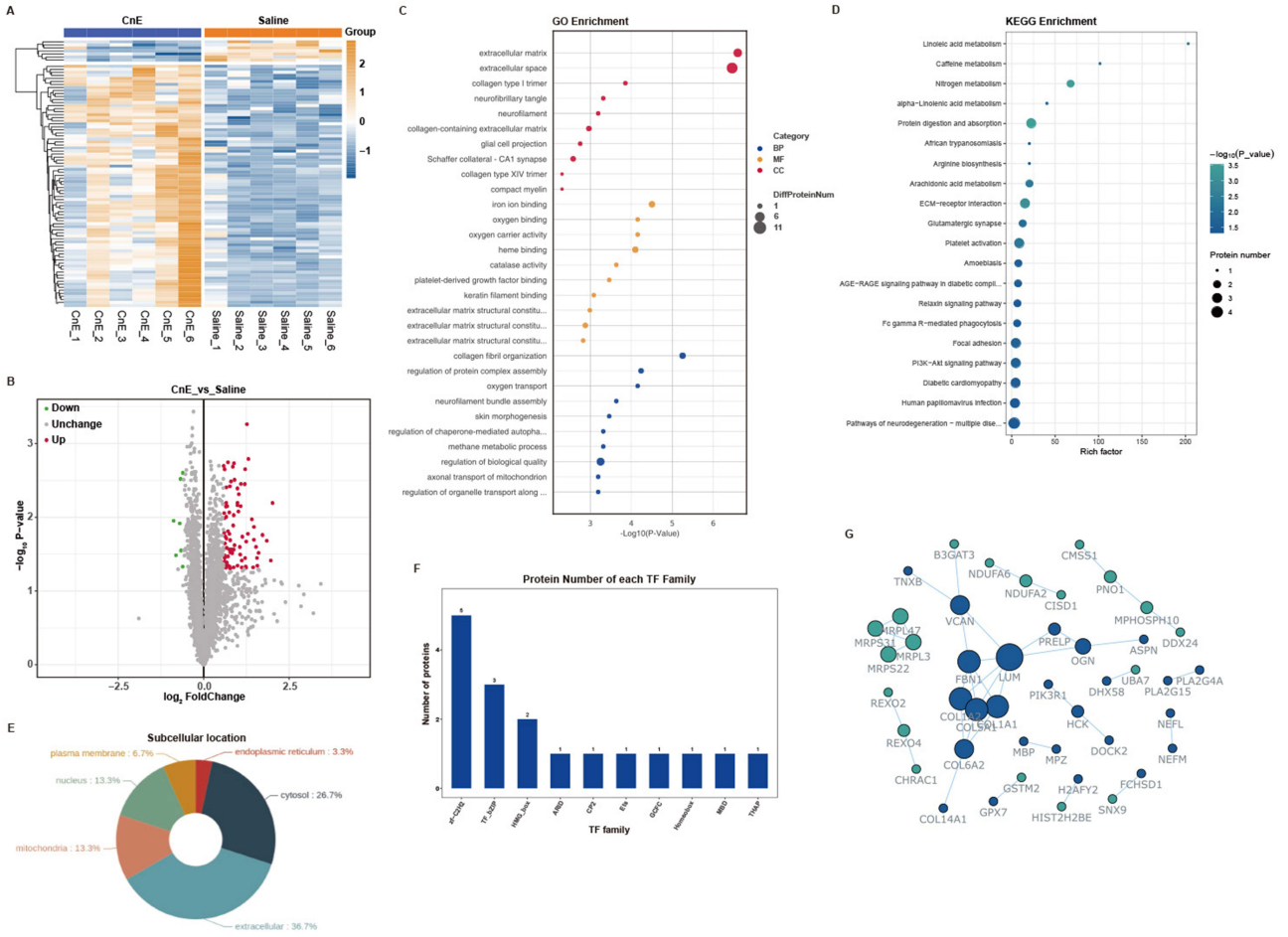

Figure 3 Analysis of differentially expressed proteins between saline and CnE-Treated TNBC model mice. (**A**) Heatmap of differentially expressed proteins (n=6). (**B**) Volcano plot of differentially expressed proteins (n=6). (**C**) GO enrichment analysis of differentially expressed proteins. (**D**) KEGG enrichment analysis of differentially expressed proteins. (**E**) Subcellular localization analysis of differentially expressed proteins. (**F**) Transcription factor family analysis of differentially expressed proteins. (**G**) PPI analysis of differentially expressed proteins.

Abbreviations: CnE, *Clinacanthus nutans* extract; TNBC, triple-negative breast cancer; GO, Gene Ontology; KEGG, Kyoto Encyclopedia of Genes and Genomes; BP, Biological Process; CC, Cell Component; MF, Molecular Function; TF, Transcription Factor; PPI, Protein-Protein Interaction.

alpha-linolenic acid metabolism, and arachidonic acid metabolism), caffeine metabolism, protein digestion and absorption, and arginine biosynthesis.

Subcellular Localization Analysis and Transcription Factor Analysis of Differentially Expressed Proteins

Subcellular localization analysis (Figure 3E) indicated that, compared to the control group, the differentially expressed proteins in the CnE group were primarily distributed in the following locations, in decreasing order: extracellular, cytosol, nucleus, mitochondria, plasma membrane, and endoplasmic reticulum.

Transcription factor analysis (Figure 3F) showed that, compared to the control group, the differentially expressed proteins in the CnE group included five transcription factors from the zf-C2H2 family, three from the TF_bZIP family, two from the HMG_box family, and one each from the ARID, CP2, Ets, GCFC, Homeobox, MBD, and THAP families.

PPI Network Analysis of Differentially Expressed Proteins

PPI network analysis, based on the STRING database and Cytoscape (Figure 3G), of the differentially expressed proteins in the CnE group compared to the control group identified 44 key proteins at the network nodes. These include LUM, COL1A1, OGN, TNXB, MBP, MPZ, NEFL, NEFM, DHX58, UBA7, HCK, PIK3R1, DOCK2, PLA2G4A, PLA2G15, and others. The differentially expressed proteins were associated with the extracellular matrix, fatty acid metabolism, cell apoptosis, ferroptosis, immune response, choline metabolism, amino acid metabolism, and inflammation. These results

suggest that CnE may promote cancer cell apoptosis and ferroptosis while enhancing the cytotoxic ability of immune cells against cancer cells, ultimately inhibiting cancer cell proliferation.

GSEA_KEGG Enrichment Analysis of Differentially Expressed Proteins

The previous results indicate that CnE affects tumors involved in multiple pathways. To distill and identify the primary gene sets influenced by CnE, we conducted a GSEA KEGG enrichment analysis. The findings suggest that, compared to the control, CnE upregulates several gene sets, including focal adhesion, calcium signaling pathway, glycerophospholipid, long term depression, long term potentiation, axon guidance, insulin signaling pathway, GNRH signaling pathway, leukocyte transendothelial migration, and natural killer cell mediated cytotoxicity (Figure 4A and B). These gene sets are primarily associated with extracellular matrix dynamics, calcium signaling, neural activity, glucose metabolic regulation, and immune modulation. This suggests that CnE may inhibit the rapid proliferation of cancer cells by enhancing the cytotoxic capacity of immune cells. However, it is puzzling that the upregulated gene sets also involve neuronal activity, such as long-term depression, long-term potentiation, and axon guidance.

In contrast, CnE downregulates gene sets such as aminoacyl tRNA biosynthesis, lysine degradation, tryptophan metabolism, base excision repair, cysteine and methionine metabolism, mismatch repair, fatty acid metabolism, glycolysis gluconeogenesis, nucleotide excision repair, RNA degradation, and DNA replication compared to the control (Figure 4C and D). These gene sets mainly pertain to amino acid metabolism, nucleic acid repair, and nucleic acid stabilization. Notably, cysteine and methionine are crucial for cancer cell proliferation, and reducing their levels could help suppress cancer cell expansion. Additionally, robust nucleic acid repair is a primary factor in cancer cell drug resistance, so downregulating this repair and stabilization mechanism could be beneficial for patients facing drug resistance.

Analysis of Differentially Expressed Protein Levels

To investigate the impact of CnE on the expression levels of key proteins, we explored the differences in protein expression induced and suppressed by CnE (Figure 5). The proteins with significantly differential expression ($P < 0.001$) include CYGB and OGN (Figure 5A). Those with $P < 0.01$ are MBP, XDH, HAL, PLA2G4A, PTGIS, DPT, ITPK1, CAMK1, TNXB, and INTS9, while the proteins with $P < 0.05$ are MRC1, NEFM, ATP2A3, and NEFL.

Furthermore, regarding the proteins whose expression is inhibited by CnE, those with $P < 0.01$ include MRPS31, GSTM2, UBA7, ENPP4, and H2BC21 (Figure 5B). Proteins with $P < 0.05$ are SURF1 and REXO4.

Pan-Cancer Prognostic Analysis of Proteins Upregulated by CnE

To assess the prognostic impact of CnE-induced proteins on the TNBC model mice, we conducted a pan-cancer prognostic analysis of these differentially expressed proteins using The Human Protein Atlas website. The results of the analysis (Figure 6) indicate that MBP, MRC1, ATP2A3, CYGB, ITPK1, and INTS9 are associated with favorable prognosis in kidney renal clear cell carcinoma. XDH and TNXB show a beneficial prognostic effect in liver hepatocellular carcinoma, while ATP2A3 is advantageous for head and neck aquamous cell carcinoma, TNXB is beneficial for ovarian serous cystadenocarcinoma, and INTS9 is favorable for glioblastoma multiforme.

Therefore, we infer that the proteins MBP, MRC1, ATP2A3, CYGB, ITPK1, INTS9, XDH, and TNXB, which are upregulated by CnE, may contribute to improved prognosis in TNBC model mice and are significant factors in CnE's ability to inhibit tumor proliferation.

Histopathology of Subcutaneous Tumors in TNBC Model Mice

Impact of CnE on Tumor Cell Morphology

To assess the effect of CnE on tumor cell morphology, hematoxylin and eosin (HE) staining was performed in this study. Histopathological analysis using HE staining (Figure 7A) revealed disorganized, densely packed clusters of tumor cells with poorly defined boundaries, extensive pathological mitosis, mild necrosis, and varying degrees of vacuolation in the saline group. In contrast, the CnE group exhibited smaller nuclear atypia, a lower nuclear-to-cytoplasmic ratio, less

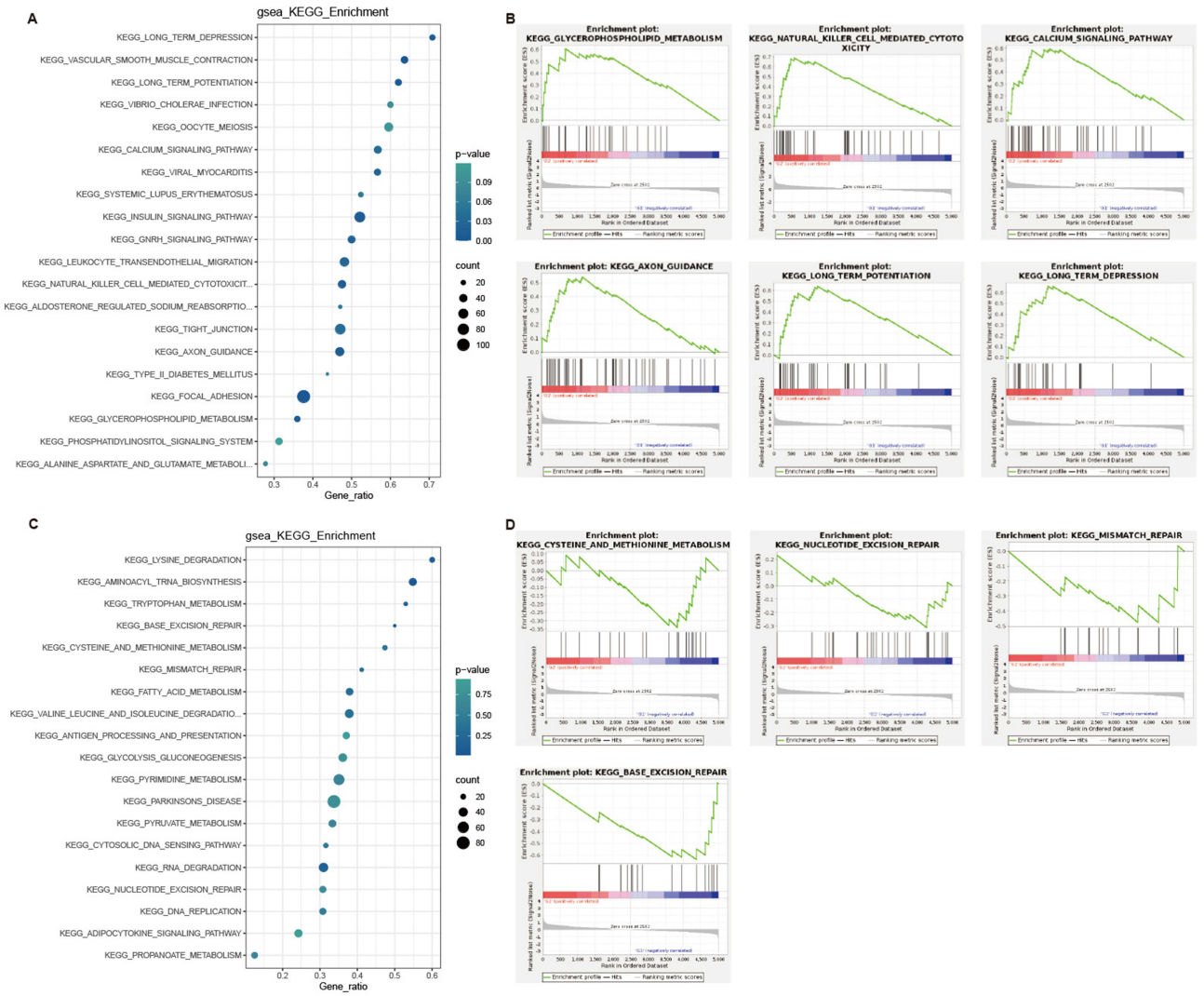

Figure 4 GSEA KEGG enrichment analysis of differentially expressed proteins between saline and CnE-treated TNBC model mice. (**A**) GSEA KEGG enrichment analysis of differentially expressed proteins upregulated by CnE. (**B**) Enrichment plots for gene sets upregulated by CnE. (**C**) GSEA KEGG enrichment analysis of differentially expressed proteins downregulated by CnE. (**D**) Enrichment plots for gene sets downregulated by CnE.
Abbreviations: CnE, *Clinacanthus nutans* extract; TNBC, triple-negative breast cancer; GSEA, Gene Set Enrichment Analysis; KEGG, Kyoto Encyclopedia of Genes and Genomes.

prominent nucleoli, and reduced mitotic activity. Notably, extensive necrosis, karyopyknosis, hyperchromasia, nuclear fragmentation, and increased apoptosis were observed in the extract-treated group.

Effect of CnE on Tumor Cell Apoptosis in TNBC Model Mice

To explore whether CnE influences apoptosis in breast cancer cells, a TUNEL assay was implemented in this study. The CnE group demonstrated a significant increase in tumor cell apoptosis compared to the saline group ($P < 0.001$; Figure 7B and C). Thus, CnE effectively promotes apoptosis in breast cancer cells, thereby suppressing their proliferation.

Effects of CnE on ATP2A3, PLA2G4A, and ITPK1 Protein Expression

To further validate the effects of CnE on the expression of ATP2A3, PLA2G4A, and ITPK1 proteins, immunohistochemical staining was employed in this study. Immunohistochemical analysis of xenograft tumors (Figure 7D, F, H) indicated that ATP2A3 expression was primarily localized to the cytoplasm and nucleus, while PLA2G4A and ITPK1 were confined to the cytoplasm. The CnE-treated group exhibited increased positive staining for ATP2A3 (1.3-fold, p <

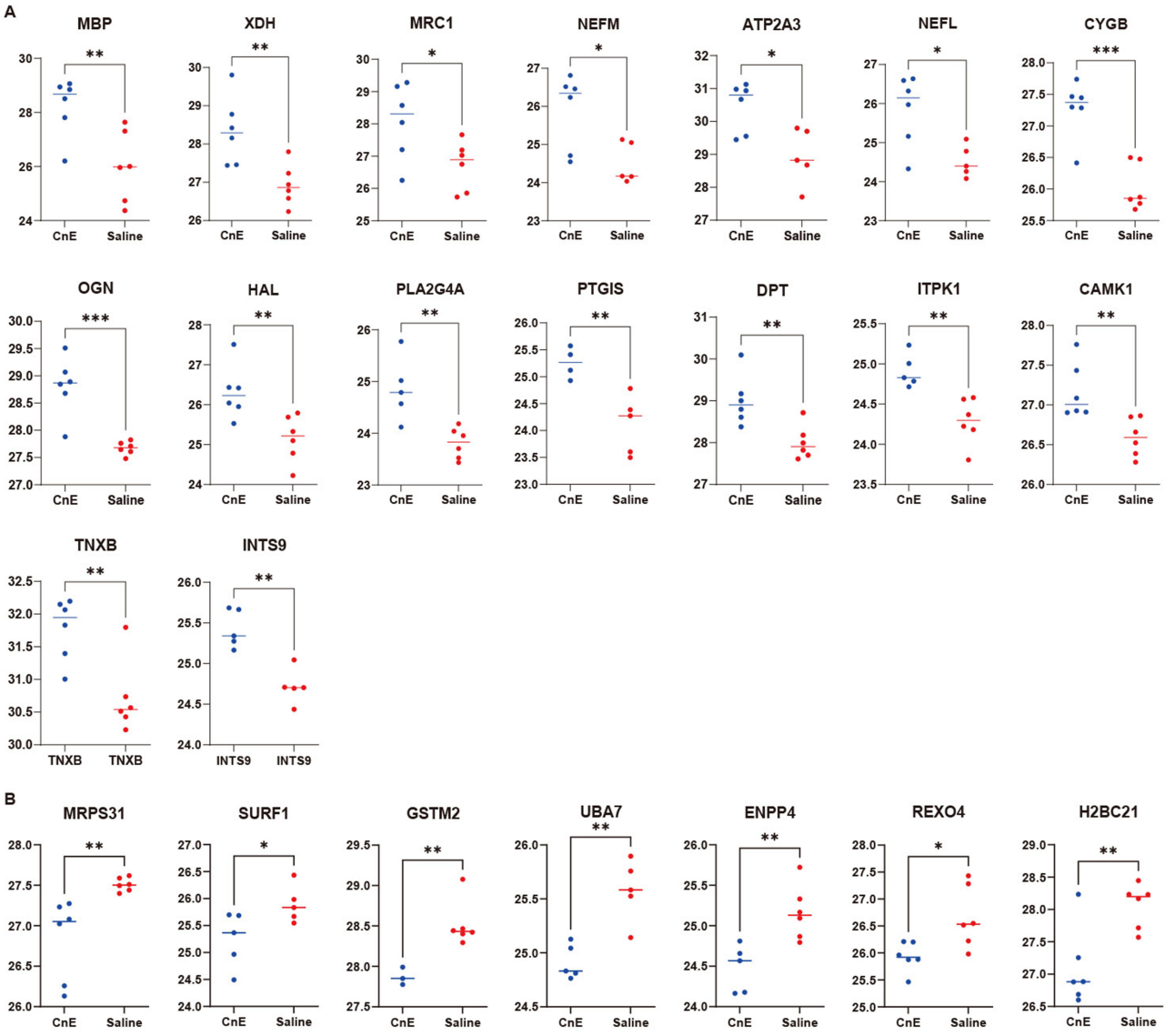

Figure 5 Analysis of differentially expressed protein levels between saline and CnE-Treated TNBC model mice. (**A**) Differentially expressed proteins that are upregulated by CnE. (**B**) Differentially expressed proteins that are downregulated by CnE. Data are presented as mean ± SEM. Statistical significance was determined using an unpaired, two-tailed Student's *t*-test. **P* < 0.05, ***P* < 0.01, ****P* < 0.001.

Abbreviations: CnE, *Clinacanthus nutans* extract; TNBC, triple-negative breast cancer.

0.05), PLA2G4A (1.6-fold, p < 0.05) and ITPK1 (3.2-fold, p < 0.01) (Figure 7E, G, I) compared to the control group (P < 0.05). These findings further corroborate the results from the proteomics study in this research, indicating that CnE can indeed inhibit the proliferation of subcutaneous tumors in TNBC model mice.

Discussion

TNBC is characterised by aggressive progression, a high likelihood of visceral metastasis (particularly to the liver, brain and lungs) and the absence of definitive therapeutic targets. Current treatments, including chemotherapy and immunotherapy, yield limited efficacy. TNBC is also unresponsive to traditional endocrine therapy and anti-HER2–targeted treatments, highlighting the need for novel, effective therapies to address this clinical challenge.[14] Traditional Chinese medicine, a long-standing therapeutic resource in China, offers unique advantages in cancer treatment because of its multi-target, multi-component nature, high efficacy and minimal side effects. Traditional Chinese medicine has emerged as a vital complement and alternative to conventional cancer therapies.[11] Evidence from existing studies has

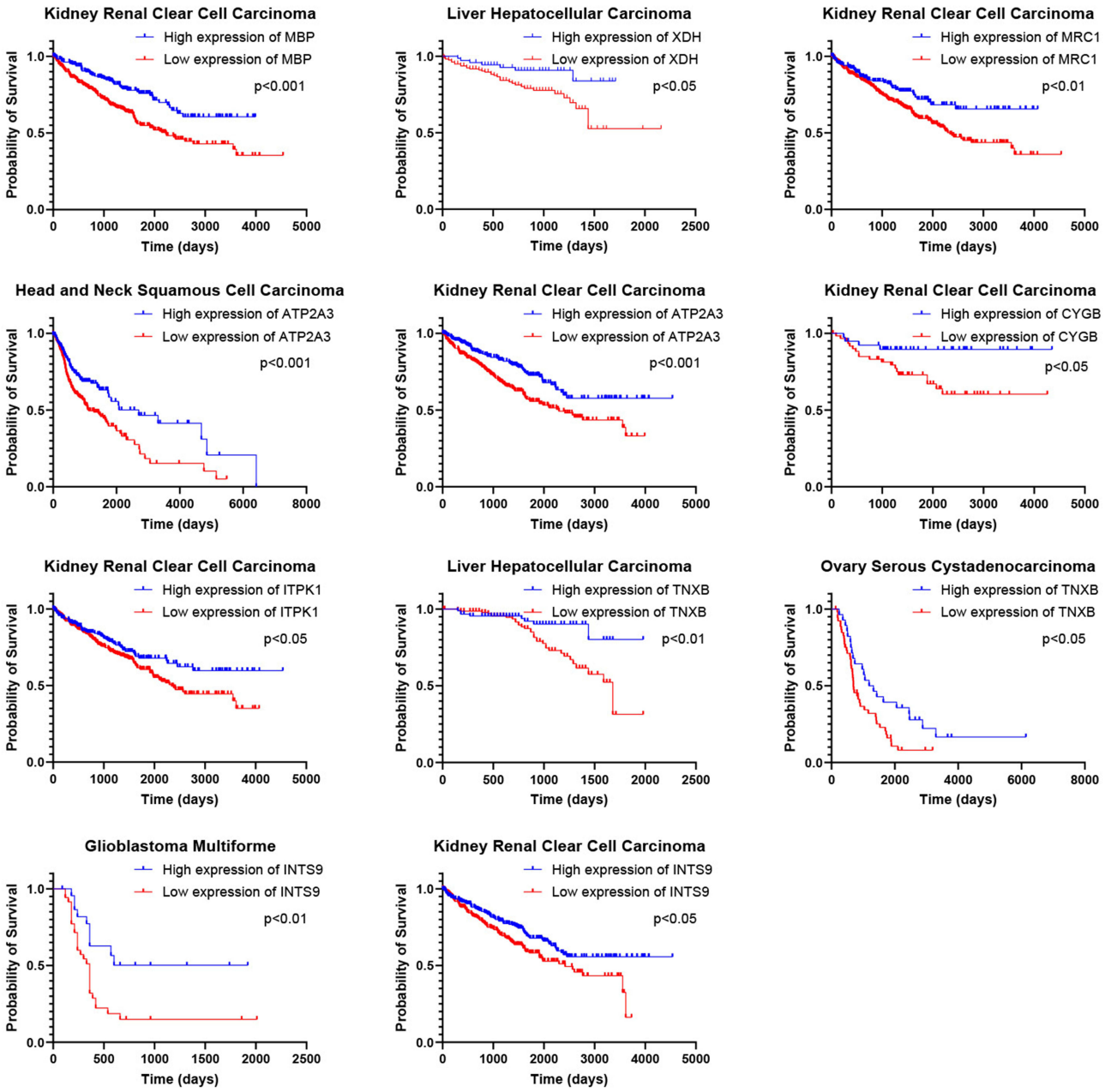

Figure 6 Pan-cancer prognostic analysis of proteins upregulated by CnE in subcutaneous tumors of TNBC model mice. Data are presented as mean ± SEM. Statistical significance was determined using an unpaired, two-tailed Student's *t*-test.
Abbreviations: CnE, *Clinacanthus nutans* extract;TNBC, triple-negative breast cancer.

demonstrated the ability of traditional Chinese medicine and its active components to inhibit breast cancer cell proliferation and promote apoptosis.[11] Modern pharmacological experiments have indicated that *C. nutans* can suppress cell proliferation, invasion and metastasis, possibly due to its bioactive constituents, such as triterpenoids, flavone C-glycoside, glucosides and glucosinolates.[7,8] However, its mechanisms of action against TNBC remain unexplored.

This study investigated the anti-cancer effects of CnE on TNBC. The extract significantly inhibited the proliferation of TNBC cell lines (MDA-MB-231 and MDA-MB-468) in a concentration-dependent manner. Using triple-negative breast cancer mouse subcutaneous xenograft model, we found that the extract markedly suppressed tumour growth and promoted tissue necrosis. To elucidate its mechanisms, we performed data-independent acquisition–based quantitative proteomic analysis of xenograft tumours. Compared with the control group, 87 differentially expressed proteins were

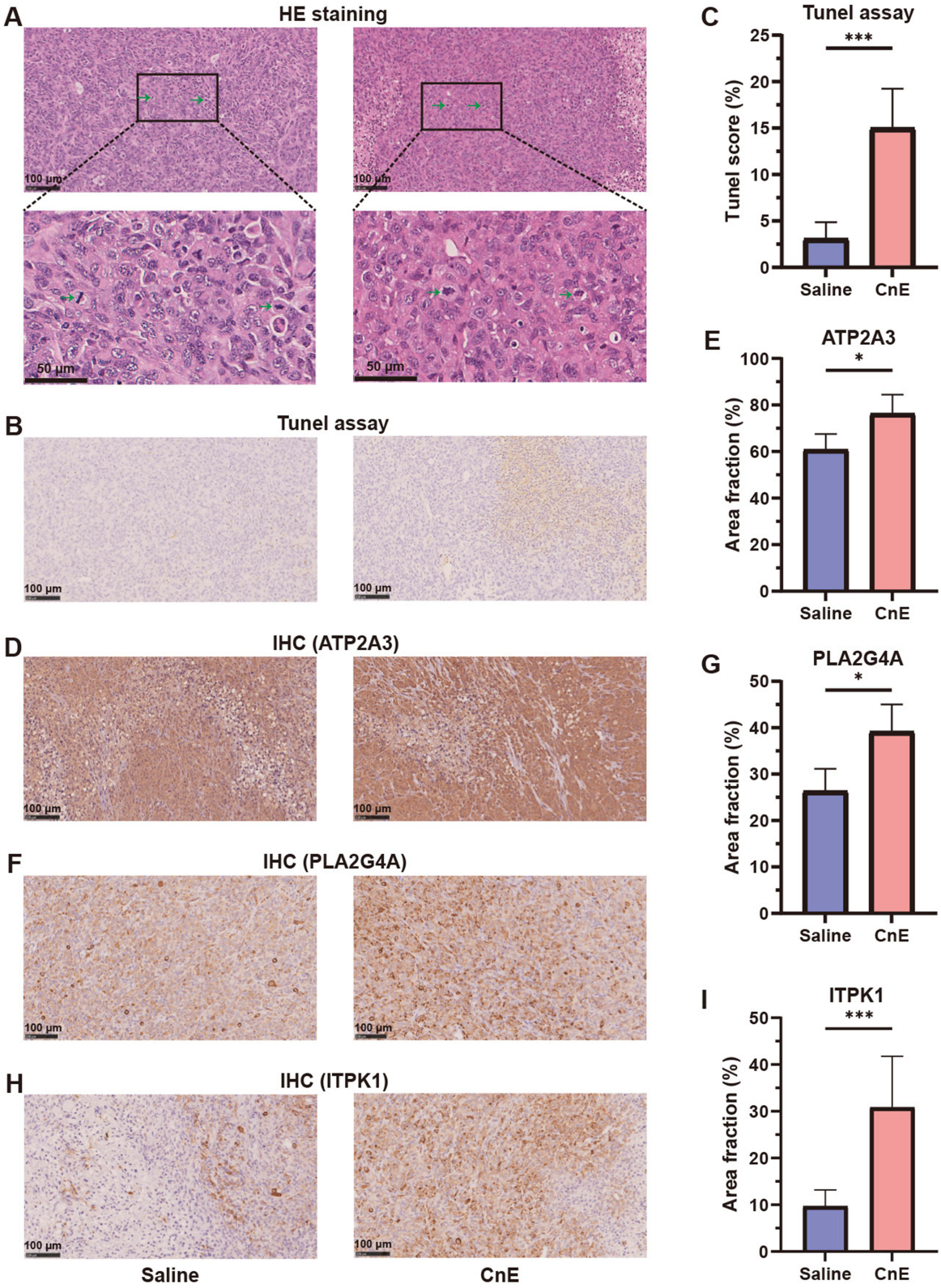

Figure 7 Effects of CnE on Histopathology of Subcutaneous Tumors in TNBC Model Mice. (**A**) HE staining. (**B**) TUNEL assay. (**C**) Statistical analysis of the TUNEL assay (n=5). (**D**) IHC assay of ATP2A3. (**E**) Statistical analysis of the IHC assay for ATP2A3 (n=5). (**F**) IHC assay of PLA2G4A. (**G**) Statistical analysis of the IHC assay for PLA2G4A (n=5). (**H**) IHC assay of ITPK1. (**I**) Statistical analysis of the IHC assay for ITPK1 (n=5). Data are presented as mean ± SEM. Statistical significance was determined using an unpaired, two-tailed Student's *t*-test. **P* < 0.05, ****P* < 0.001.

Abbreviations: CnE, *Clinacanthus nutans* extract; TNBC, triple-negative breast cancer; HE, hematoxylin and eosin; IHC, immunohistochemistry.

https://doi.org/10.2147/BCTT.S528242

identified in the CnE group, including 80 and 7 upregulated and downregulated proteins, respectively. These proteins are enriched in various cellular biological processes and signalling pathways. Next, Expression analysis, pan-cancer prognostic analysis, and histopathological analysis of ATP2A3, PLA2G4A, and ITPK1 were conducted in subcutaneous tumors induced by CnE in the TNBC model mice. Their potential roles in these tumors were inferred, suggesting that they may inhibit tumor cell proliferation and promote macrophage phagocytosis of cancer cells.

CnE May Inhibit Tumor Cell Proliferation in Breast Cancer Cells

CnE May Promote Apoptosis in Breast Cancer Cells

ATP2A3, a magnesium-dependent enzyme, catalyzes the hydrolysis of ATP coupled with Ca^{2+} transport. Its expression is induced by resveratrol, which triggers apoptosis and alters intracellular Ca^{2+} levels in breast cancer cell lines.[15] Our proteomic data indicate that ATP2A3 expression is significantly induced by CnE (Figure 5A). Pan-cancer prognostic analysis shows that ATP2A3 has a favorable prognostic effect in head and neck squamous cell carcinoma and kidney renal clear cell carcinoma (Figure 6). The TUNEL assay in this study demonstrated that CnE significantly induces apoptosis in breast cancer cells (Figure 7B and C). IHC staining further confirms that the expression of ATP2A3 is significantly induced by CnE (Figure 7D and E). Based on this information, we infer that CnE may promote apoptosis in breast cancer cells by inducing ATP2A3 expression.

CnE May Induce Ferroptosis in Breast Cancer Cells

Xanthine dehydrogenase (XDH) catalyzes the oxidation of hypoxanthine to xanthine and subsequently xanthine to uric acid, involved in contributing to the generation of reactive oxygen species (ROS).[16] Our proteomic data indicate that the expression of XDH is significantly induced by CnE (Figure 5A). Pan-cancer prognostic analysis reveals that XDH has a favorable prognostic effect in liver hepatocellular carcinoma (Figure 6). Thus, high expression levels of XDH are significantly associated with better prognosis and increased overall survival in breast cancer patients.[16]

Cytosolic phospholipase A2α (cPLA2α), including PLA2G4A, is a class of Ca^{2+}-dependent enzymes that catalyze the release of fatty acids from phospholipids, preferentially hydrolyzing sn-2 arachidonic acid to initiate the release of arachidonic acid (AA), which produces lipid mediators.[17] Xu et al reported that PLA2G4A is involved in ferroptosis in triple-negative breast cancer.[17] Our proteomic data indicate that PLA2G4A expression is significantly induced by CnE (Figure 5A). IHC staining further confirms that the expression of PLA2G4A is significantly induced by CnE (Figure 7F and G).

The ROS generated by XDH, combined with the AA induction through the PLA2G4A and the presence of intracellular free iron, creates all the necessary conditions for inducing ferroptosis. Therefore, we conclude that CnE induces ferroptosis in breast cancer cells by promoting the expression of XDH and PLA2G4A, thereby inhibiting cancer cell proliferation.

CnE May Induce Necroptosis in Breast Cancer Cells

ITPK1 is a cytosolic kinase that generates higher-order inositol polyphosphates.[18] Recent findings indicate that ITPK1 kinase activity is essential for executing cytokine-induced necroptosis mediated by mixed lineage kinase domain-like (MLKL).[18] Additionally, ITPK1 sensitizes IgA-mediated target cell killing in vivo, enhancing IgA-dependent neutrophil killing of Her2-positive CD47-deficient murine target cells.[19] Previous studies have demonstrated that ITPK1 and Inositol polyphosphate multikinase (IPMK) regulate TNF-α-mediated necroptosis in human cancer cell lines in vitro through the production of inositol phosphates, a process that also involves receptor-interacting serine/threonine kinase 3 and MLKL.[18] In this study, proteomic data indicate that CnE significantly induces the expression of ITPK1 (Figure 5A). Pan-cancer prognostic analysis revealed that ITPK1 has a beneficial prognostic effect in kidney renal clear cell carcinoma (Figure 6). IHC staining further confirms that CnE significantly enhances ITPK1 expression (Figure 7H and I). Therefore, we propose that CnE upregulates ITPK1 expression, leading to necroptosis in breast cancer cells and thereby inhibiting cancer cell proliferation.

CnE Inhibits Breast Tumor Cell Proliferation Through Other Mechanisms

OGN[20] and DPT[21] have been shown to inhibit cell proliferation and invasiveness in breast cancer by targeting the PI3K/AKT/mTOR signaling pathway. Our study found that CnE induces OGN and DPT, thereby suppressing cancer cell proliferation through the same pathway.

Furthermore, DNA methylation-mediated silencing of neurofilament genes NEFH, NEFM,[22,23] and NEFL[22] is frequently associated with the progression of breast cancer and potentially other malignancies through the Wnt/β-catenin signaling pathway. Our findings indicate that CnE-induced NEFM and NEFL might inhibit cancer cell proliferation by suppressing this signaling pathway.

Additionally, CYGB is recognized as a potential tumor suppressor in breast cancer, which is epigenetically suppressed. CYGB inhibits breast cancer through mechanisms involving glucose intake and metabolism by targeting GLUT1 and HXK2 in both p53-dependent and independent manners,[24] and as well as inhibiting the PI3K/AKT/mTOR pathway.[25] Our study revealed that CnE-induced CYGB inhibits cancer cell proliferation by suppressing the GLUT1/HXK2 signaling pathway.

MBP-1 functions as a double-edged sword, inhibiting both primary and metastatic tumor growth while modulating matrix metalloproteinase expression, thereby presenting therapeutic potential against breast cancer progression. MBP-1 has been shown to inhibit breast cancer growth and metastasis in immunocompetent mice.[26] Our research indicates that CnE-induced MBP suppresses cancer cell proliferation by inhibiting MMP activity.

CnE May Promote Tumor Cell Proliferation in Breast Cancer Cells

The mannose receptor C-type 1 (MRC1) is an endocytic lectin receptor primarily expressed in immune cells, such as macrophages and dendritic cells.[27] The functions of MRC1 include the clearance of endogenous molecules, promotion of antigen presentation, and regulation of cell activation and transport.[27] The high expression of MRC1 may be positively

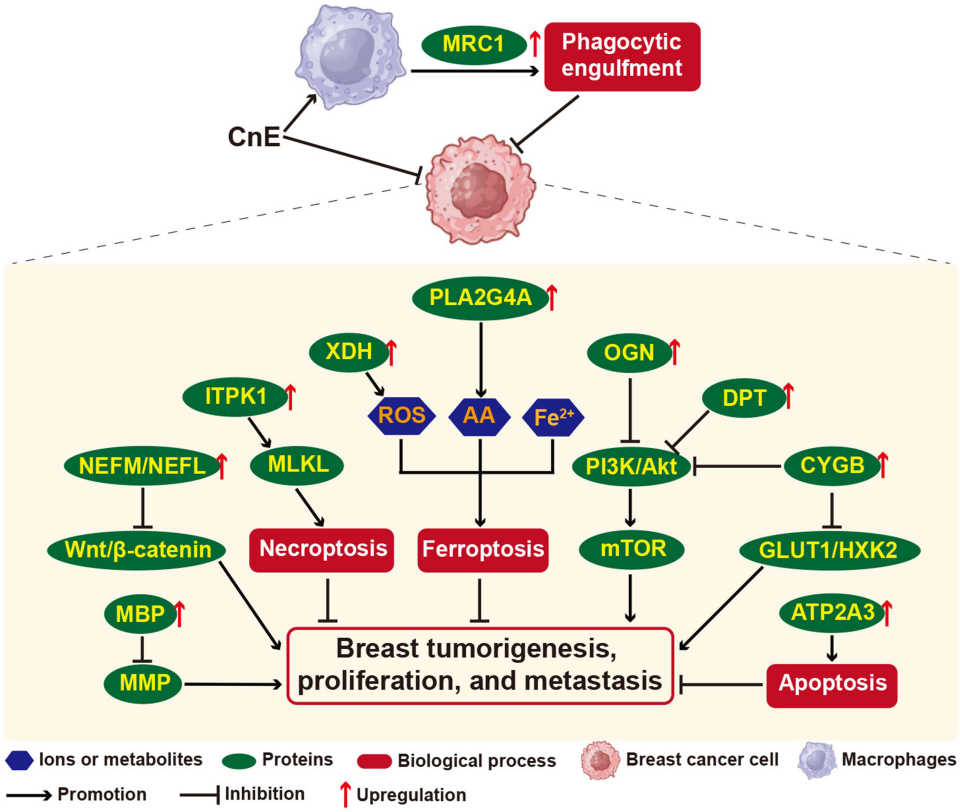

Figure 8 The molecular mechanism by which CnE inhibits subcutaneous tumor proliferation in TNBC model mice is illustrated.
Abbreviations: CnE, *Clinacanthus nutans* extract; TNBC, triple-negative breast cancer.

https://doi.org/10.2147/BCTT.S528242

correlated with immune infiltration, particularly in adrenocortical carcinoma, breast invasive carcinoma, cervical squamous cell carcinoma, and endocervical adenocarcinoma. Additionally, MRC1 expression is positively associated with factors that enhance immunotherapy efficacy while negatively correlating with certain potential barriers.[28] Its association with immune checkpoint molecules underscores MRC1's role in the tumor immune microenvironment.[28] In this study, proteomic data indicate that CnE significantly induces the expression of MRC1 (Figure 5A). Pan-cancer prognostic analysis revealed that ITPK1 has a beneficial prognostic effect in kidney renal clear cell carcinoma (Figure 6). Therefore, we propose that CnE upregulates ITPK1 expression, leading to necroptosis in breast cancer cells and thereby inhibiting cancer cell proliferation.

Based on all the preceding information, we propose a potential molecular mechanism by which CnE inhibits the proliferation of subcutaneous tumors in a TNBC mouse model (Figure 8). This mechanism primarily involves two aspects: on one hand, CnE promotes the infiltration of immune cells to kill and phagocytose cancer cells; on the other hand, CnE induces apoptosis, ferroptosis, and necroptosis in breast cancer cells, thereby inhibiting tumor cell proliferation. However, the specific molecular mechanisms by which CnE exerts these two effects remain unclear and require further exploration and study in the future.

Conclusion

CnE shows promise in reducing TNBC cell viability, inhibiting proliferation, and promoting apoptosis, ferroptosis, and necroptosis, mediated through its multifaceted effects on cellular processes and signaling pathways. ATP2A3, PLA2G4A, and ITPK1 are key targets of its anti-tumor activity in subcutaneous tumors in TNBC model mice. CnE enhances the immune response of TNBC model mice against cancer cells, including their ability to kill and phagocytose cancer cells. Currently, the exploration of these targets is still in its preliminary stages, and many targets and related pathways require further validation. Additionally, the complexity of the in vivo tumor microenvironment necessitates more investigation into the precise regulatory effects of CnE on these proteins. Future studies should aim to elucidate the mechanisms by which ATP2A3, PLA2G4A, and ITPK1 protein expression is modulated, as well as their interactions with upstream and downstream pathways in TNBC development.

Funding

Hainan Medical University 2025 Academic Enhancement Support Program Project(XSTS2025068), Joint Project on Health Science and Technology Innovation in Hainan Province (WSJK2024MS197), Key R&D Project of Hainan Provincial Department of Science and Technology (ZDYF2020139, ZDYF2018158), Hainan Provincial Natural Science Foundation (823MS138) and College Student Innovation and Entrepreneurship Training Program Project (X202311810097).

Disclosure

The authors report no conflicts of interest in this work.

References

1. Bray F, Laversanne M, Sung H, et al. Global cancer statistics 2022: GLOBOCAN estimates of incidence and mortality worldwide for 36 cancers in 185 countries. *CA Cancer J Clin*. 2024;74(3):229–263. doi:10.3322/caac.21834
2. Zhang Y, Zhang D, Meng Q, et al. Precision treatment exploration of breast cancer based on heterogeneity analysis of lncRNAs at the single-cell level. *BMC Cancer*. 2021;21(1):918. doi:10.1186/s12885-021-08617-7
3. Wolff AC, Somerfield MR, Dowsett M, et al. Human epidermal growth factor receptor 2 testing in breast cancer: ASCO-college of American pathologists guideline update. *J Clin Oncol*. 2023;41(22):3867–3872. doi:10.1200/JCO.22.02864
4. Zheng C, Liu Y, Wang X, et al. Clinical efficacy and biomarker analysis of neoadjuvant camrelizumab plus chemotherapy for early-stage triple-negative breast cancer: a experimental single-arm Phase II clinical trial pilot study. *Int J Surg*. 2024;110(3):1527–1536. doi:10.1097/JS9.0000000000001011
5. Sakdarat S, Shuyprom A, Pientong C, et al. Bioactive constituents from the leaves of Clinacanthus nutans Lindau. *Bioorg Med Chem*. 2009;17(5):1857–1860. doi:10.1016/j.bmc.2009.01.059
6. Chia TY, Gan CY, Murugaiyah V, et al. A narrative review on the phytochemistry, pharmacology and therapeutic potentials of Clinacanthus nutans (Burm. f.) Lindau leaves as an alternative source of future medicine. *Molecules*. 2021;27(1):139. doi:10.3390/molecules27010139

7. Lin CM, Chen -H-H, Lung C-W, et al. Recent advancement in anticancer activity of Clinacanthus nutans (Burm. f.) Lindau. *Evid Based Complement Alternat Med*. 2021;2021:5560502. doi:10.1155/2021/5560502
8. Lin CM, Chen HH, Lung CW, Chen HJ. Antiviral and immunomodulatory activities of Clinacanthus nutans (Burm. f.) Lindau. *Int J Mol Sci*. 2023;24(13):10789.
9. Yong YK, Tan JJ, Teh SS, et al. Clinacanthus nutans extracts are antioxidant with antiproliferative effect on cultured human cancer cell lines. *Evid Based Complement Alternat Med*. 2013;2013:462751. doi:10.1155/2013/462751
10. Zakaria Y, Abdullah H, Abdullah H. Cytotoxicity of Clinacanthus nutans and mechanism of action of its active fraction towards human cervical cancer cell line, HeLA. *Jurnal Sains Kesihatan Malaysia*. 2018;16(2):39–50. doi:10.17576/jskm-2018-1602-06
11. Yuan J, Liu Y, Zhang T, et al. Traditional Chinese medicine for breast cancer treatment: a bibliometric and visualization analysis. *Pharm Biol*. 2024;62(1):499–512. doi:10.1080/13880209.2024.2359105
12. Ghasemzadeh A, Nasiri A, Jaafar H, et al. Changes in phytochemical synthesis, chalcone synthase activity and pharmaceutical qualities of Sabah snake grass (Clinacanthus nutans L.) in relation to plant age. *Molecules*. 2014;19(11):17632–17648. doi:10.3390/molecules191117632
13. Cui TW, Lu L-F, Cao X-D, et al. Exosomes combined with biosynthesized cellulose conduits improve peripheral nerve regeneration. *IBRO Neurosci Rep*. 2023;15:262–269. doi:10.1016/j.ibneur.2023.09.009
14. Mai N, Chen J-F, Rana S, et al. Pathologic complete response to KEYNOTE522 and HER2-directed therapy for synchronous TNBC and HER2+ breast cancer. *NPJ Precis Oncol*. 2024;8(1):162. doi:10.1038/s41698-024-00631-9
15. Izquierdo-Torres E, Hernández-Oliveras A, Meneses-Morales I, et al. Resveratrol up-regulates ATP2A3 gene expression in breast cancer cell lines through epigenetic mechanisms. *Int J Biochem Cell Biol*. 2019;113:37–47. doi:10.1016/j.biocel.2019.05.020
16. Alwahsh M, Hamadneh Y, Marchan R, et al. Glutathione and Xanthine metabolic changes in tamoxifen resistant breast cancer cell lines are mediated by down-regulation of GSS and XDH and correlated to poor prognosis. *J Cancer*. 2024;15(13):4047–4058. doi:10.7150/jca.96659
17. Xu S, Tuo Q-Z, Meng J, et al. Thrombin induces ferroptosis in triple-negative breast cancer through the cPLA2α/ACSL4 signaling pathway. *Transl Oncol*. 2024;39:101817. doi:10.1016/j.tranon.2023.101817
18. Dovey CM, Diep J, Clarke BP, et al. MLKL requires the inositol phosphate code to execute necroptosis. *Mol Cell*. 2018;70(5):936–948.e7. doi:10.1016/j.molcel.2018.05.010
19. Richterich CA, Logtenberg MEW, Jansen MJH, et al. ITPK1 sensitizes tumor cells to IgA-dependent neutrophil killing in vivo. *J Immunol*. 2024;213(8):1244–1254. doi:10.4049/jimmunol.2300372
20. Xu T, Zhang R, Dong M, et al. Osteoglycin (OGN) inhibits cell proliferation and invasiveness in breast cancer via PI3K/Akt/mTOR signaling pathway. *Onco Targets Ther*. 2019;12:10639–10650. doi:10.2147/OTT.S222967
21. Su Y, Du Y, Ye S, et al. Clinical importance and PI3K/Akt pathway-dependent anti-proliferative role of PALMD and DPT in breast canc1er. *Pathol Res Pract*. 2023;249:154717. doi:10.1016/j.prp.2023.154717
22. Calmon MF, Jeschke J, Zhang W, et al. Epigenetic silencing of neurofilament genes promotes an aggressive phenotype in breast cancer. *Epigenetics*. 2015;10(7):622–632. doi:10.1080/15592294.2015.1050173
23. Li D, Zhao W, Zhang X, et al. NEFM DNA methylation correlates with immune infiltration and survival in breast cancer. *Clin Clin Epigenet*. 2021;13(1):112. doi:10.1186/s13148-021-01096-4
24. Feng Y, Wu M, Li S, et al. The epigenetically downregulated factor CYGB suppresses breast cancer through inhibition of glucose metabolism. *J Exp Clin Cancer Res*. 2018;37(1):313. doi:10.1186/s13046-018-0979-9
25. Demirci S, Doğan A, Apdik H, et al. Cytoglobin inhibits migration through PI3K/AKT/mTOR pathway in fibroblast cells. *Mol Cell Biochem*. 2018;437(1–2):133–142. doi:10.1007/s11010-017-3101-2
26. Kanda T, Raychoudhuri A, Steele R, et al. MBP-1 inhibits breast cancer growth and metastasis in immunocompetent mice. *Cancer Res*. 2009;69(24):9354–9359. doi:10.1158/0008-5472.CAN-09-2974
27. Martinez-Pomares L. The mannose receptor. *J Leukoc Biol*. 2012;92(6):1177–1186. doi:10.1189/jlb.0512231
28. Wu Z, Huang C. Unveiling the impact of MRC1 on immune infiltration and patient's prognosis: a pan-cancer analysis based on single-cell and bulk sequencing. *Int J Gen Med*. 2024;17:2575–2592. doi:10.2147/IJGM.S461144